Word count: 4631
Tables: 4
Figures: 3

# Tractography-based segmentation of the corpus callosum reveals a reduced relationship to cortical white matter volume in young children with developmental delay

Carissa Cascio, PhD, Martin Styner, PhD, Rachel G Smith, BA, Michele D Poe, PhD, Guido Gerig, PhD, Heather C Hazlett, PhD, Matthieu Jomier, MS, Roland Bammer, PhD, and Joseph Piven*, MD

*To whom correspondence should be addressed:
Joseph Piven, MD
Department of Psychiatry
CB# 3367
University of North Carolina
Chapel Hill, NC 27599-3367

The authors acknowledge support of this work by NIH grant HD03110 (J Piven). We also wish to acknowledge Sean Ho for the original segmentation software, Daniel Reuckert for affine registration tools, and Sarang Joshi for the fluid registration program.

## Abstract

Objective: The corpus callosum is the primary anatomical substrate for interhemispheric communication, which is important for a range of adaptive and cognitive behaviors in early development. Previous studies that have measured the corpus callosum in developmental populations have been limited by the use of rather arbitrary methods of subdividing the corpus callosum. Our goal was to measure the corpus callosum in a sample of developmentally delayed children using a subdivision that more accurately reflected the anatomical properties of the corpus callosum. Method: We apply tractography to subdivide the corpus callosum into regions corresponding to the cortical regions to and from which its fibers travel in a sample of very young children with developmental delay (DD), a precursor to general mental retardation, in comparison with typically developing (TD) children. Results: The data demonstrate that the midsagittal area of the entire corpus callosum is reduced in children presenting with developmental delay, reflected in the smaller area of each of the fiber-based callosal subdivisions. In addition, while the area of each subdivision was strongly and significantly correlated with the corresponding cortical white matter

volume in controls, this correlation was prominently absent in the developmentally delayed sample. Conclusion: A fiber-based subdivision successfully separates lobar regions of the corpus callosum and the areas of these regions distinguish a developmentally delayed clinical group from controls. This distinction was evident both in the area measurements themselves, and in their correlation to the white matter volumes of the corresponding cortical lobes.

## Introduction

The corpus callosum (CC) is the largest commissural fiber tract in the brain, and serves to connect homologous cortical regions between the two hemispheres. This fiber tract is considered the most important anatomical substrate for interhemispheric communication, which is crucial for a range of human behaviors from motor skills such as bimanual coordination to cognitive skills such as visual attention and reading. The anatomical and functional integrity of this group of pathways that relay information from cortical areas to their contralateral homologues critically impacts the development of these and other behaviors.

Developmental studies have established that the CC has an extended growth trajectory that continues throughout childhood and adolescence. Cross-sectional as well as longitudinal studies indicate that the size of the CC increases dramatically in the first two years after birth (1) and continues to increase substantially throughout childhood and adolescence (2-4). Development appears to follow an anterior-posterior trajectory, with size increasing earlier in the more anterior regions of the CC, and later in

the more posterior regions (5). It is interesting to note that this is the inverse of the well-known posterior-anterior pattern of development in the cerebral cortex.

Developmental delay (DD) is a diagnosis given to very young children who perform below the average range on tests of adaptive behavior. This poor performance is often a precursor to a diagnosis of mental retardation at an older age, when IQ can be reliably assessed. Developmental delay can be associated with a specific syndrome, such as Fragile X, or can be non-syndromic, and thus considered to be of polygenic or epigenetic origin.

The neuroanatomical substrates of developmental delay have yet to be elucidated. The CC is a viable candidate as a contributor to generalized developmental delay, as a compromise in interhemispheric communication would have global effects on a range of adaptive behaviors. Differences in overall CC size or variability of CC size have been observed in samples of children with a variety of disorders of which developmental delay (DD) is a feature (1, 6-10), but the results have been mixed and difficult to interpret. Additionally, differences in CC size have been demonstrated in

syndromic groups that do not have associated DD/MR, such as high-functioning autism (11,12). Only one study has included a sample of children with nonsyndromic DD (1). In addition to global measurement of the entire CC, many of these studies have achieved a degree of anatomical specificity by dividing the midsagittal CC area into smaller units and measuring those subregions separately.

The most common method used to divide the CC into subregions is the Witelson method (13). This method divides the CC into seven subregions with an initial division into anterior and posterior halves, and subsequent divisions determined by further geometric ratios or anatomical landmarks in the curve of the structure (Figure 2a). The subdivisions are generally thought to correspond roughly to cortical regions to which their fibers project, but the accuracy of such an assumption is dubious given the fairly arbitrary, geometric nature of the subdivision method.

Diffusion tensor imaging (DTI) can be used to predict probable fiber trajectories in white matter tracts such as the CC. This technique, called tractography, produces a representation of the most probable trajectories and concentration of white matter fibers

connecting two regions of interest (ROIs). Recently, it has been demonstrated that tractography can be used as a tool to subdivide the midsagittal CC according to the cortical targets of its fibers (14-16). This type of subdivision separates the CC into more physiologically relevant components than geometric subdivisions like the Witelson method, and allows the subdivisions more potential to be interpreted in light of behaviors associated with their different cortical regions.

In this study we use this novel tractography-based method to subdivide the CC. Rather than using subjective, artificially imposed boundaries as in the Witelson method (Figure 2a), our method segments the CC into truly anatomically relevant regions by using fibers from cortical targets as guides for making divisions. Additionally, instead of hard boundaries, our method uses a probabilistic subdivision that is better suited for a functionally heterogeneous structure such as the CC (16). In this study, our goal was to use this technique to compare a group of children with generalized developmental delay to a control sample on the following variables: midsagittal callosal area, area of four

fiber-derived callosal subregions, and correlation between the areas of subregions to the corresponding lobe white matter volumes.

## Methods

### Subjects

13 children aged 18-40 months with general developmental delay (DD) were included. This sample represents children who are likely to be diagnosed with non-syndromic mental retardation at an age when IQ can be reliably assessed. 14 age-matched, typically developing (TD) control children were also included. The DD group was recruited from selected regional state Children's Developmental Services Agencies (CDSAs). TD children were recruited from community advertisements. All DD subjects had a diagnosis of developmental delay and were identified on the basis of CDSA evaluation scores. Their CDSA and medical records were screened to ensure that there was no identifiable cause for their delay (e.g. prematurity, genetic or neurological disorder, CNS injury, perinatal trauma) and had no indication of a pervasive developmental disorder, or a sibling with autism. This medical record screening was

supplemented with a telephone screening interview administered to the parents. Study approval was acquired from the UNC and Duke Institutional Review Boards and written informed consent was obtained from the parent or guardian of each subject.

Descriptive statistics can be found in Table 1.

## Clinical Assessment

All subjects were administered a battery of measures including the Mullen Scales of Early Learning (17), the Vineland Adaptive Behavior Scales (18), Preschool Language Scale 4$^{th}$ edition (19), behavioral rating scales, and a standardized neurodevelopmental examination, and screened for autism with the Childhood Autism Rating Scale (20). Medical records were reviewed in order to screen for indication of pervasive developmental disorder. Diagnosis of DD was confirmed using the Mullen Scales of Early Learning and the Vineland Adaptive Behavior Scale; subjects scoring <75 on both instruments were included.

## Image acquisition

All scans were acquired on a 1.5 T GE Sigma Advantage MR scanner. T1-weighted structural images were acquired using a 3D IR prepped SPGR protocol with a 256x256x124 image matrix at 0.78125 x 0.78125 x1.5 mm resolution. DTI images were acquired using 4 repetitions of a 12-direction spin-echo single-shot echo planar imaging (EPI) sequence with a 128x128x30 image matrix at 2x2x4 mm resolution using a b-value of 1000 s/mm$^2$. Total scan time was approximately 45 minutes. TD children were scanned at night while sleeping; DD children were sedated for the scan following the standard pediatric sedation protocol at the hospital, under the supervision of a pediatric anesthesiologist.

### DTI Preprocessing

Each DTI slice was screened for motion and other artifacts using a custom software program designed to automatically detect and handle slices or shots that fall outside predetermined parameters. After cleaning, both the correction of eddy-current based image distortions using mutual information based unwarping and the calculation of the diffusion tensor elements as well as metrics and the eigensystem (i.e.

eigenvectors and –values) derived from them were performed using another customized software package. The tensor parameters derived from this step were used in our tractography program to compute fiber maps (21).

### Segmentation of the corpus callosum from surrounding brain tissue

The CCs were segmented from the T1-weighted structural image with the in-house developed CC segmentation tool using a using a 2D Fourier descriptor-based active shape model segmentation (22). Based on a prior automatic tissue segmentation, the initial values for position, scale and grayscale normalization were computed automatically. From these initial values, the CC segmentation was performed in 2 steps: first using a fully constrained CC model contour segmentation in a large search region, then secondly using an unconstrained contour segmentation in a smaller search region. During each step a CC contour model is adapted iteratively until convergence. This segmentation scheme establishes a point-to-point correspondence at the contour between all segmented CC's. It is fully automatic and 100% reproducible. In an additional stability study, the coefficient of variance of the segmented CC area across

different images of the same subject on different scanners (23) was measured at 2.7%. That study thus confirmed the high stability and reliability of our segmentation scheme.

### Creation of subdivision template using tractography

The T1-weighted anatomical images of five subjects, selected from our sample on the basis of image quality, were parcellated into four cortical lobes: occipital, parietal, temporal, and frontal. Subjects from both groups were included in the template generation sample. Using the left and right lobes of the parcellation maps for these cases as regions of interest (ROIs), probable fiber trajectories were traced (using an automated, locally developed tractography program) between the midsagittal plane of the CC (source) and the lobar ROIs (targets). Thus we divided the CC into four segments defined by the fibers that projected to each of the four lobes. Because a very small number of fibers projected to the temporal and occipital lobes in our images, and because there was a good deal of overlap between them, fibers from the occipital lobe were combined with fibers from the temporal lobe to result in one occipitotemporal CC

subdivision. Conversely, because a very large number of fibers were found that projected to the frontal lobe, fibers from the frontal lobe were manually divided into those coming from the anterior and posterior frontal lobe to result in an anterior frontal and a posterior frontal CC subdivision (see Figure 1a). Based on these four fiber maps (Figure 1b), a probabilistic CC subdivision model was computed automatically. Each point of the contour of the CC was assigned a probability of belonging to each of the four subdivisions using the closest distances to produce the final subdivision template. The probabilistic subdivision used is contrasted to a hard subdivision by its assignment of multiple labels with probabilistic weights to each point rather than a forced assignment of each point to a single label. This is ideal for the CC because of the spatial overlap of its commissural pathways.

### Corpus callosum subdivision by application of template to remainder of sample

The corpus callosa of the remaining subjects were subdivided using this template (16). The subdivision was propagated to each CC contour using the template's point-to-point correspondence with the CC segmentations. The probability of each point within

the CC belonging to a certain subdivision was then computed as that of its nearest contour point. CCs subdivided with the template are illustrated in Figure 2b. The resulting areas of each of the four CC subregions were measured, and added together to produce the total CC area. The volumes of the total brain, total gray tissue, total white tissue, and each of the four cortical lobes had been previously measured (24; Hazlett et al., submitted) and were used in the analyses to determine the relationships between the CC, its fiber-based subdivisions, and the cortical lobes.

## Statistics

A mixed model for repeated measures was used to examine group differences in corpus collosum size. Each subject had 4 observations, one per sub-area of the CC. An unstructured covariance matrix was used to estimate the within-subject correlations. This allowed each CC sub-area to have a freely estimated variance and covariance with the other observations. The model regressed group, age, gender, CC region, and group X CC region, on CC area. Total brain volume (TBV) was added as a covariate. The regression coefficient for the group indicates the mean difference between DD and

TD subjects, while the group x CC region interaction tests whether this difference varies significantly across regions. An estimate of the group difference in total CC size was estimated based on the estimates for the 4 sub-areas.

In order to examine differences in the correlation between the CC area and TBV and cerebral white matter volumes, partial correlations between CC area and TBV and cerebral white matter volumes, controlling for age and gender, were estimated for both TD and DD subjects. As a follow-up analysis to evaluate possible regional differences in the relationship between CC area and white matter volume, the partial correlations between the CC sub-area and the corresponding regional white matter volume were estimated for each group.

## Results

Table 2 presents the differences in CC area between the DD subjects and the control subjects. The midsagittal area of the full CC was significantly smaller in the developmentally delayed group than in the control group (Diff = -.50, p= .011). Additionally, each of the four fiber-based subdivisions of the CC (anterior frontal,

posterior frontal, occipitotemporal, and parietal) was smaller in the developmentally delayed group than the control group. This difference remained after adjusting for group differences in total brain volume (Table 3).

Table 4 presents the correlations between CC subareas and total brain volume (TBV) and total white tissue. Analyses were focused on white tissue since there was a stronger relationship expected between CC area and cerebral white tissue. For the control group, the area of the CC was significantly correlated with total white tissue volume. The DD group showed no evidence of correlations between CC area and TBV or total white tissue volume. Figure 3 shows the raw data and the mean trends between total CC area and total white matter volume.

Follow-up analyses examined the relationship between the sub-areas of the CC and their corresponding white matter lobe volumes (Table 4). The areas of the CC subdivisions and their corresponding lobar white matter volumes were strongly and significantly correlated in the typically developing group at the $p \leq 0.05$ level (see Table 4), but not in the developmentally delayed group.

## Discussion

We have shown that nonspecific developmental delay (DD) is associated with robust abnormalities in the CC. We demonstrate reduced midsagittal CC area in DD, and strikingly reduced correlations between CC subdivision areas and their corresponding cortical lobe volumes. In the control group, the area of each fiber-based CC subregion was significantly positively correlated with the volume of white matter in its corresponding lobe. There is a remarkable lack of such significant relationships in the DD group. This suggests an anatomical nonspecificity in developmental delay, i.e. there may be a disconnection between the fibers in the CC and the cortical lobes between which they travel. Such nonspecificity may serve to render interhemispheric connections less efficient. The combination of reduced interhemispheric connection as evidenced by the reduced CC area and this nonspecificity between the CC subareas and their cortical targets could create a drastically reduced substrate for information transfer between hemispheres.

Our area results are consistent with those of Njiokiktjien et al. (1), who demonstrated reduced callosal size in severe learning disability/mental retardation. This smaller area was regionally nonspecific: each of the four fiber-based CC subdivisions were consistently smaller in the DD group. This is in contrast to previous studies of children whose delay was of a specific, known etiology, in which area differences were concentrated in particular regions of the CC. For example, Schmitt et al. (9) and Tomaiuolo et al. (10) both found a greater reduction of CC area in the posterior half of the structure in Williams syndrome. This is consistent with the visual spatial deficits seen in this disorder, as visual spatial processing is largely mediated by posterior cortex in the occipital and parietal lobes. Similarly, Preis and colleagues' (7) study of developmental language disorder, although demonstrating no significant differences, revealed a trend toward altered anterior CC area, corresponding to the frontal and anterior temporal cortices which mediate language processing.

In addition, these data validate the method of using tractography to subdivide the CC. This is a novel method and we submit that is of considerable value in adding to

and improving the vast literature on the CC and providing a more physiologically meaningful way to subdivide it. In addition, the method is more stable than previous methods in that it is automatically rather than manually applied, and probabilistic rather than hard-decision-based. It is noteworthy that this new method was successfully used to distinguish a clinical group from a control group, in a way that was fairly dramatic, especially considering the relatively small size of our sample.

This small sample size is one of the primary limitations of this study. DD without a genetic or otherwise identifiable etiology is relatively rare, and this limits both the power of the study and our ability to extrapolate the results to other clinical groups that exhibit MR. Another significant limitation is the difficulty in assessing cognitive ability reliably in such young children. This highlights the importance of replication at older ages.

Future directions will include repeating this analysis in the same sample at a time point two years after their initial assessment, as part of an ongoing longitudinal study, to determine the trajectory of CC development in DD relative to control children. The

deficits characterized as delay in our young sample are likely to be precursors to mental retardation (MR), which will be more clearly manifest and more easily measured when the children are older. In addition, at the time of follow-up it would be of significant benefit to conduct an age-appropriate battery of tests for functional laterality (i.e. handedness, dichotic listening, etc.) in this sample. The addition of these data would be valuable in assessing the relationship between anatomical abnormalities in the CC and the behavioral and cognitive profiles with which they are associated in DD/MR. It would be of great interest to conduct some of these laterality tests using fMRI to assess any differences in related neural activity, although even with the best training methods available, this would most likely have to be done with an older population. The disconnection we demonstrate between CC fibers and their cortical targets may not be specific to the CC. It may simply be an index of a more general disconnection of projecting axons in the brains of delayed individuals. It will be important to use other applications of DTI in combination with structural MRI to elucidate the relationships between other groups of projecting axons and their targets in the brains of this sample

of children with DD. Finally, although the methodology we use in this study is not adequate to determine whether the differences in CC area can be attributed to fewer fibers, less myelination, or smaller fiber diameter, it would be extremely instructive to devise experiments to begin to distinguish between these possibilities.

## References


1. Njiokiktjien C, de Sonneville L, Vaal J. 1994. Callosal size in children with learning disabilities. *Behavioral Brain Research* 64: 213-218.

2. Giedd JN, Rumsey JM, Castellanos FX, Rajapakse JC, Kaysen D, Vaituzis AC, Vauss YC, Hamburger SD, and Rapoport JL. 1996. A quantitative MRI study of the copus callosum in children and adolescents. *Developmental Brain Research* 91: 274-280.

3. Giedd JN, Blumenthal J, Jeffries NO, Rajapakse JC, Vaituzis AC, Liu H, Berry YC, Tobin M, Nelson J, and Castellanos FZ. 1999. Development of the human corpus callosum during childhood and adolescence: a longitudinal MRI study. *Progress in Neuopsychopharmacology and Biological Psychiatry* 23: 571-588.

4. Keshavan MS, Diwadkar VA, DeBellis M, Dick E, Kotwal R, Rosenberg DR, Sweeney JA, Minshew N, and Pettegrew JW. 2002. Development of the corpus callosum in childhood, adolescence and early adulthood. *Life Sciences* 70: 1909-1922.

5. Thompson PM, Giedd JN, Woods RP, MacDonald D, Evans AC, and Toga AW. 2000. Growth patterns in the developing brain detected by using continuum mechanical tensor maps. *Nature* 404: 190-192.

6. Manes F, Piven J, Vranic D, Nanclares V, Plebst C, and Starkstein SE. 1999. An MRI study of the corpus callosum and cerebellum in mentally retarded autistic individuals. *Journal of Neuropsychiatry and Clinical Neurosciences* 11: 470-474.

7. Preis S, Steinmetz H, Knorr U, and Jancke L. 2000. Corpus callosum size in children with developmental language disorder. *Cognitive Brain Research* 10: 37-44.

8. Shashi V, Muddasani S, Santos CC, Berry MN, Kwapil TR, Lewandowski E, and Keshavan MS. 2004. Abnormalities of the corpus callosum in nonpsychotic children with chromosome 22q11 deletion syndrome. *NeuroImage* 21: 1399-1406.

9. Schmitt JE, Eliez S, Warsofsky IS, Bellugi U, Reiss AL. 2001. Corpus callosum morphology of Williams syndrome: Relation to genetics and behavior. *Developmental Medicine and Child Neurology* 43: 155-159.

10. Tomaiuolo F, Di Paola M, Caravale B, Vicari S, Petrides M, and Caltagirone C. 2002. Morphology and morphometry of the corpus callosum in Williams syndrome: A T1-weighted MRI study. *Neuroreport* 13: 2281-2284.

11. Piven J, Bailey J, Ranson BJ, and Arndt SA. 1997. An MRI study of the corpus callosum in autism. *American Journal of Psychiatry* 154: 1051-1056

12. Hardan AY, Minshew NJ, and Keshavan MS. 2000. Corpus callosum size in autism. *Neurology* 55(7): 1033-1036.

13. Witelson SF. 1989. Hand and sex differences in the isthmus and genu of the human corpus callosum, a postmortem biological study. *Brain* 112: 799-835.

14. Abe O, Masutani Y, Aoki S, Yamasue H, Yamada H, Kasai K, Mori H, Hayashi N, Masumoto T, and Ohtomo K. 2004. Topography of the human corpus callosum using diffusion tensor tractography. *Journal of Computer Assisted Tomography* 28: 533-539.

15. Huang H, Zhang J, Jiang H, Wakana S, Poetscher L, Miller MI, van Zijl PCM, Hillis AE, Wytic R, and Mori S. 2005. DTI tractography based parcellation of white matter: Application to the mid-sagittal morphology of corpus callosum. *NeuroImage* 26: 195-205.

16. M. Styner, R. Gimpel Smith, C. Cascio, I. Oguz, M. Jomier M. 2005. Corpus callosum subdivision based on a probabilistic model of Inter-hemispheric connectivity. *Medical Image Computing and Computer Assisted Interventions* LNCS 3750: 765-772.

17. Mullen EM. *Mullen Scales of Early Learning AGS Edition.* American Guidance Service, Inc. USA: 1995.

18. Sparrow SS, Balla DA, and Cicche HV. *Vineland Adaptive Behavior Scales-Interview Edition Survey Form Manual,* Circle Pines: American Guidance Service, Inc; 1984.

19. Zimmerman IL, Steiner VG, and Pond RE. Preschool Language Scale-Fourth Edition (PLS-IV). Psychological Corporation; 2002.

20. Mesibov GB, Schopler E, Schaffer B, Michal N. 1989. Use of the childhood autism rating scale with autistic adolescents and adults. *Journal of the American Academy of Child and Adolescent Psychiatry.* 28 (4): 538-541.

21. Fillard P, Gilmore J, Lin W, Piven J, and Gerig G. 2003. Quantitative analysis of white matter fiber properties along geodesic paths. Lecture Notes in Computer Science LNCS #2879, Medical Image Computing and Computer Assisted Interventions 2003, pp.16-23.

22. Szekely G, Kelemen A, Brechbuhler C, and Gerig G. 1996. Segmentation of 2-D and 3-D objects from MRI volume data using constrained elastic deformations of flexible Fourier contour and surface models. *Medical Image Analysis* 1(1): 19-34

23. Styner M, Charles HC, Park J, Lieberman J, and Gerig G 2002. Multi-site validation of image analysis methods: Assessing intra and inter-site variability. *SPIE Medical Imaging 2002: Image Processing* 4684: 278-286.

24. Hazlett HC, Poe MD, Gerig G, Smith RG, Provenzale J, Ross A, Gilmore JH, Piven J. An MRI and Head Circumference Study of Brain Size in Autism: Birth through Age Two Years. *Archives of General Psychiatry* (in press).

## Figures and tables

### Figure 1a. Manual split of anterior and posterior frontal fibers

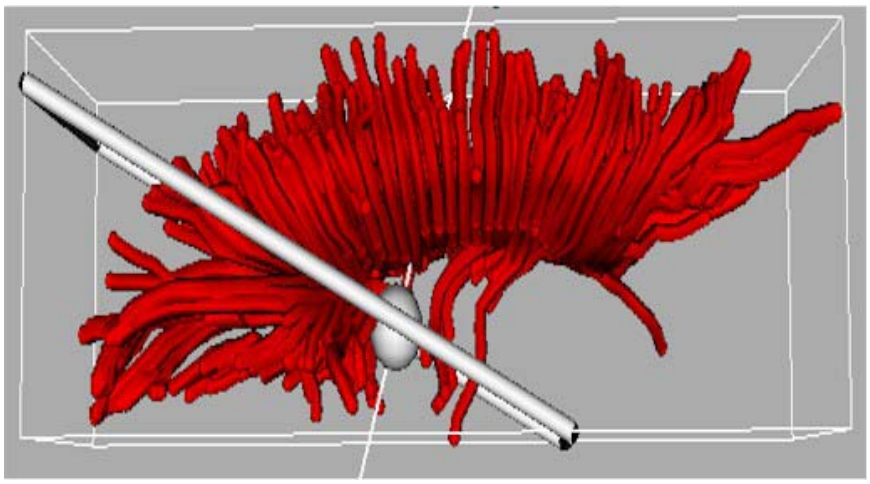

Figure 1a. A plane was rotated manually to divide the frontal fibers into the smaller group of more anteriorly-projecting fibers and the larger group of more posterior/superiorly-projecting fibers.

Figure 1b. Fibers between midsagittal CC and cortical lobes

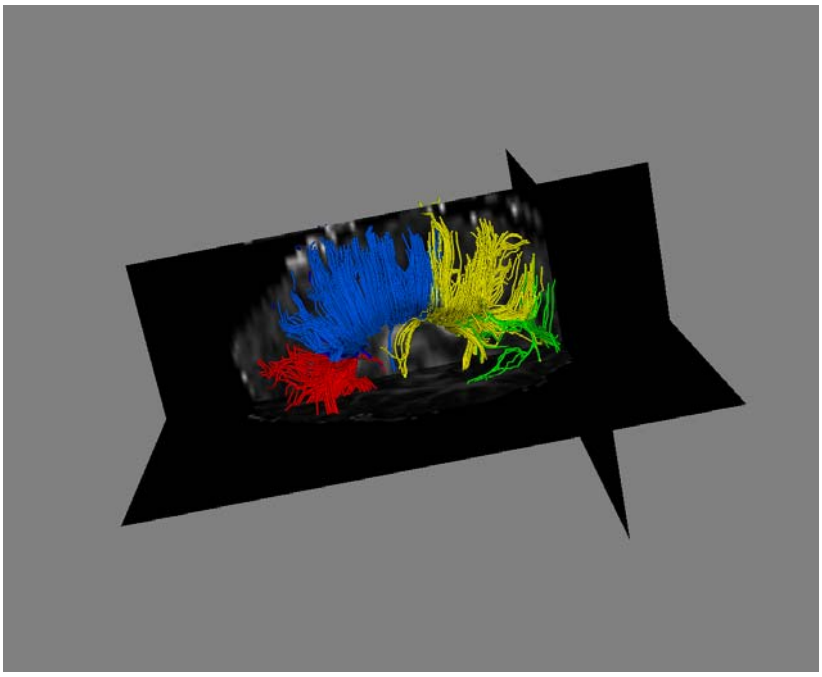

Figure 1b. Fibers traced from CC for template using frontal, parietal, and occipito-temporal volumes as ROIs. The frontal fibers were split manually into anterior (red) and posterior (blue). Parietal fibers shown in yellow; occipito-temporal fibers in green. The CC areas under these fibers for 5 cases were then used as a template to apply to the rest of the sample for subdivision of the CC.

Figure 2a: Witelson subdivision method

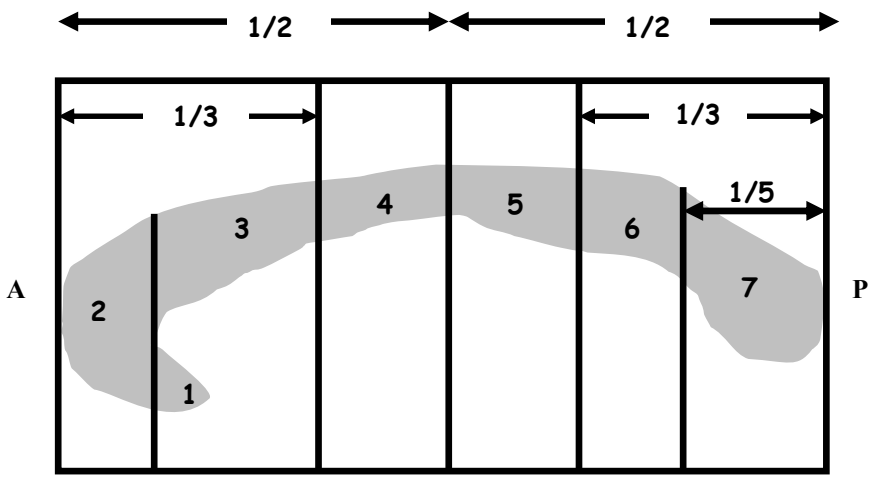


Figure 2a. The Witelson subdivision method. The midsagittal corpus callosum is bounded and divided into halves. The bounding box is then divided into thirds. These two divisions create subregions 2-5. Subregions 6 and 7 are created by dividing the bounding box into fifths; area 7 is the posterior-most fifth of the structure. Subregion 1 is separated from subregion 2 by a vertical line placed flush with the curve of the genu. (Adapted from Witelson, 1989).

Figure 2b: Probabilistic subdivision model for each of the four lobar subdivisions

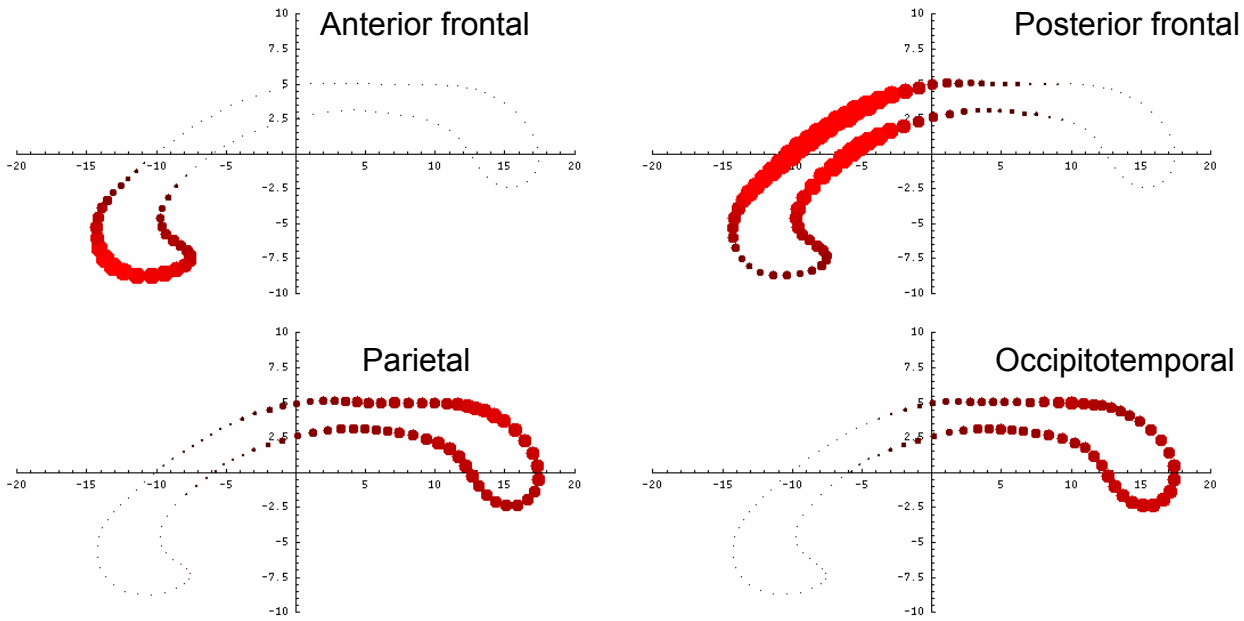


Figure 2b. Probabilistic subdivision model (average of 6 representative cases): Size and brightness of each point along the CC contour represents the probability of its assignment to the given lobar subdivision.

Figure 3: Total CC area vs. total white tissue

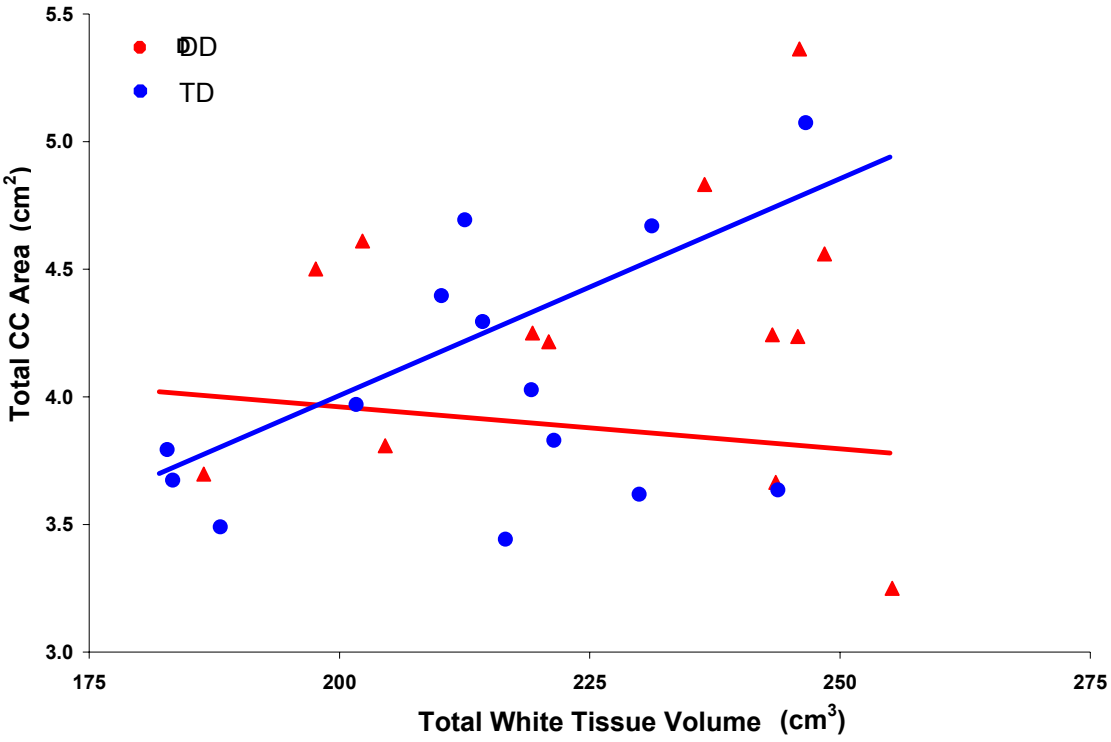


Figure 3. Relationship between total white tissue volume and total CC area for the developmentally delayed group (red) and the control group (blue).

## Table 1. Subject information

| | DD (N=13) | | | TD (N=14) | | |
|---|---|---|---|---|---|---|
| **Variable** | **Mean** | **SD** | **Range** | **Mean** | **SD** | **Range** |
| **Age (years)** | 2.8 | 0.4 | 1.9 - 3.4 | 2.2 | 0.4 | 1.6 - 3.2 |
| **IQ (Mullen score)** | 56.1 | 6.7 | 49.0 - 68.0 | 105.2 | 18.7 | 70.0 - 140.0 |
| **Male** | 62% | | | 64% | | |

## Table 2. Corpus Callosum Area, Subdivisions, and Brain Volumes

| | DD (N=13) | | | TD (N=14) | | |
|---|---|---|---|---|---|---|
| **Corpus Callosum Area ($cm^2$)** | **Mean** | **SD** | **Range** | **Mean** | **SD** | **Range** |
| **Total** | 3.90 | 0.39 | 3.24 - 4.68 | 4.35 | 0.56 | 3.48 - 5.35 |
| **Anterior Frontal** | 0.54 | 0.08 | 0.40 - 0.71 | 0.59 | 0.10 | 0.42 - 0.75 |
| **Posterior Frontal** | 1.41 | 0.15 | 1.07 - 1.64 | 1.52 | 0.18 | 1.17 - 1.78 |
| **Occipital-Temporal** | 0.86 | 0.10 | 0.70 - 1.02 | 0.98 | 0.13 | 0.75 - 1.23 |
| **Parietal** | 1.10 | 0.14 | 0.87 - 1.31 | 1.27 | 0.17 | 0.94 - 1.59 |
| **Brain Volumes ($cm^3$)** | | | | | | |
| **TBV** | 1165 | 87 | 952 - 1300 | 1154 | 120 | 970 - 1304 |
| **TCWV** | 222 | 20 | 186 - 255 | 219 | 25 | 183 - 248 |
| **Frontal** | 92.9 | 10.0 | 80.0 - 108.5 | 90.5 | 11.8 | 73.3 - 106.0 |
| **Occipital-Temporal** | 58.6 | 5.4 | 48.9 - 67.4 | 57.6 | 6.5 | 48.2 - 67.0 |
| **Parietal** | 70.2 | 6.1 | 57.6 - 84.9 | 71.1 | 7.4 | 59.5 - 83.4 |

(TBV: total brain volume, TCWV: total cerebral white volume)

Table 3. DD vs. TD for CC area.

| | Diff | SE | p |
|---|---|---|---|
| Total CC area | -0.50 | 0.18 | 0.010 |
| **Anterior Frontal** | -0.08 | 0.03 | 0.034 |
| **Posterior Frontal** | -0.11 | 0.04 | 0.016 |
| **Occipital-Temporal** | -0.15 | 0.06 | 0.016 |
| **Parietal** | -0.16 | 0.06 | 0.017 |

Adjusted for age, gender and total brain volume (TBV).

Table 4. Correlations between CC subdivisions and lobe volumes

| CC subdivision | Lobe White Matter | DD Area (p) | TD Area (p) |
|---|---|---|---|
| Total | TBV | -.31 (.33) | .54 (.05)* |
| Total | Cerebral White Matter | -.17 (.63) | .66 (.02)* |
| Anterior frontal | Frontal | .07 (.83) | .54 (.07) |
| Posterior frontal | Frontal | -.08 (.82) | .64 (.03)* |
| Occipito-temporal | Occipito-temporal | -.09 (.79) | .73 (.01)* |
| Parietal | Parietal | -.05 (.89) | .57 (.05)* |

* denotes significant correlation at $p \leq 0.05$.